Validation of SCIAMACHY Level-1 and Level-2 Products by Balloon-Borne Differential Optical Absorption Spectroscopy (DOAS)

Dorf[1], M., H. Bösch[1,5], A. Butz[1,2], C. Camy-Peyret[2], M. P. Chipperfield[3], K. Gerilowski[7], K. Grunow[4], W. Gurlit[7], H. Harder[6], S. Kühl[1], L. Kritten[1], A. Lindner[1], S. Payan[2], A. Rozanov[7], C. von Savigny[7], B. Simmes[1], C. Sioris[8], F. Weidner[1], and K. Pfeilsticker[1]

(1) Institut für Umweltphysik, University of Heidelberg, Heidelberg, Germany
(2) Laboratoire de Physique Moléculaire pour l'Atmosphère et l'Astrophysique (LPMAA), Université Pierre et Marie Curie, Paris, France
(3) Institute for Atmospheric Science, School of Earth and Environment, University of Leeds, Leeds, UK
(4) Meteorologisches Institut, Freie Universität Berlin, Berlin, Germany
(5) now with Jet Propulsion Laboratory (JPL), Pasadena, USA
(6) Max Planck Institut für Chemie, Mainz, Germany
(7) Institut für Umweltphysik und Fernerkundung, University of Bremen, Bremen, Germany
(8) Harvard-Smithsonian Center for Astrophysics, Cambridge, USA

ABSTRACT: Level 1 (Limb radiance and solar irradiance) and level 2 products (profiles of O_3, NO_2, BrO) of the Envisat/SCIAMACHY instrument have been validated by balloon-borne measurements of the same quantities using the same optical technique. The balloon-borne measurements greatly helped to obtain an accuracy of better than 5 % for the targeted level 1 products (Gurlit et al. 2005; Weidner et al. 2005). Comparison studies with preliminary level 2 retrievals are encouraging. For the individual profiles, the comparisons indicate an accuracy of ±20% for O_3 and NO_2 (Butz et al. 2006). For BrO a bias of -20% / +20% is observed for altitudes above/below 25 km, respectively (Dorf et al. 2006). The results depend on the individual species, considered wavelength range, profile height and geophysical condition of the measurements.

1. INTRODUCTION

The SCanning Imaging Absorption spectroMeter for Atmospheric CHartographY (SCIAMACHY) instrument onboard the european Envisat satellite is an UV/visible/near-IR spectrometer designed to measure direct and scattered sunlight in various viewing directions (Bovensmann et al. 1999). An exciting new feature of SCIAMACHY is to probe the atmosphere in subsequent and spatially overlapping nadir and limb scanning observations. This eventually allows to discriminate between the measured total atmospheric column amounts (nadir) and total stratospheric columns, obtained from integrated stratospheric profiles, in order to obtain tropospheric column amounts of the targeted gases (Sioris et al. 2003; Sierk et al. 2006).

Here, we briefly report on the efforts made to validate SCIAMACHY level 1 and level 2 products by balloon-borne solar occultation UV/visible spectroscopy. So far, the LPMA/DOAS payload (Limb Profile Monitor of the Atmosphere / Differential Optical Absorption Spectroscopy) has been deployed on 4 validation campaigns conducted at high, mid and low-latitudes (Table 1). For all flights, the payload was equipped with a UV/visible

Table 1: Compendium of LPMA / DOAS observations and coincident Envisat/SCIAMACHY overpasses. BA and SO indicate balloon ascent and solar occultation measurements, respectively. Adopted from Butz et al. (2006).

Balloon flight date, time/UT	Location	Geophysical condition	Available datasets	Satellite coincidence orbit, date, time/UT	Altitude range/km	Time delay/h	Spatial distance/km
04 Mar. 2003	Kiruna	high lat. spring	SO: LPMA	5273, 4 Mar., 11:05	20–30	−5.1	369–496
13:20–16:17	67.9° N, 21.1° E	SZA: 71.1°–94.1°		5285, 5 Mar., 7:17	23–24	+15.3	498–499
23 Mar. 2003	Kiruna	high lat. spring	BA: LPMA, DOAS	5545, 23 Mar., 11:07	18–28	−5.2	268–496
14.47–17:28	67.9° N, 21.1° E	SZA: 78.9°–94.7°		5558, 24 Mar., 9:01	19–29	+17.4	10–495
			SO: LPMA, DOAS	5545, 23 Mar., 11:07	20–30	−6.2	63–458
				5558, 24 Mar., 9:01	17–30	+16.0	256–453
9 Oct. 2003	Aire sur l'Adour	mid-lat. fall	BA: DOAS	8407, 9 Oct., 9:51	17–31	−6.5	738–988
15:39–17:09	43.7° N, 0.3° W	SZA: 72.0°–87.8°		8421, 10 Oct., 9:20	25–33	+17.2	547–977
24 Mar. 2004	Kiruna	high lat. spring	BA: DOAS	10798, 24 Mar., 10:35	12–33	−5.4	371–499
14:04–17:31	67.9° N, 21.1° E	SZA: 74.5°–95.3°		10812, 25 Mar., 10:04	6–16	+19.9	32–485
			SO: DOAS	10798, 24 Mar., 10:35	10–33	−6.9	191–436
				10812, 25 Mar., 10:04	10–20	+16.7	301–475
17 June 2005	Teresina	tropical winter	BA: in preparation	17240, 17 June, 11:53	25–30	−8.1	382–491
18:32–21:13	5.1° S, 42.9° W	SZA: 60.6°–95.8°		17255, 18 June, 13:02	5–33	+18.4	6–490
			SO: in preparation	17240, 17 June, 11:53	23–32	−9.1	519–971
				17255, 18 June, 13:02	8–33	+16.2	12–496

DOAS spectrometer (Ferlemann et al. 2000), a Fourier transform spectrometer (Camy-Peyret, 1995) and a mini-DOAS instrument (Weidner et al. 2005). Correlative measurements with Envisat/SCIAMACHY were performed using an air mass trajectory matching technique. For photochemically sensitive gases a suitable correction scheme was employed, in order to correct for illumination (daytime) mismatches in the individual measurements. For more details of the employed methods, techniques and scientific results see Gurlit et al. (2005), Weidner et al. (2005), Dufour et al. (2005), Canty et al. (2005), Butz et al. (2006), Dorf et al. (2006), Sioris et al. (2006), Feng et al. (2006), Frieler et al. (2006) and others.

2. METHODS

The validation studies involved the following methods and tools.

2.1 Instrumentation and trace gas retrieval:

The French/German LPMA/DOAS balloon payload comprises three optical spectrometers, which analyze direct sunlight over virtually the entire wavelength range from the UV to the mid-IR and thus essentially cover the same wavelength range as SCIAMACHY. Since 2002, additionally, a small versatile UV/visible spectrometer (referred to as 'mini-DOAS') is routinely deployed on the same gondola and observes scattered skylight in limb scattering geometry (like SCIAMACHY). Details of the setup and operational performance of the instruments are described in Camy-Peyret (1995), Ferlemann et al. (1998) and Weidner et al. (2005). Only a short description of the instrumental features important for SCIAMACHY validation is given here.

The LPMA/DOAS spectrometers are deployed on an azimuth-controlled gondola. It carries an automated sun-tracker (Hawat et al., 1998), which provides a beam of sunlight (beam diameter 10 cm) for the direct sun spectrometers. The inner core (beam diameter 5 cm) of the solar beam is directed into the LPMA Fourier Transform spectrometer (FT-IR) (effective field of view (FOV) = 0.2°). Two small telescopes (diameter = 1 cm, effective FOV = 0.53°) mounted into the beam's outer fringe, feed the collected sunlight into the two DOAS spectrometers. The optical setup guarantees that the UV/visible (DOAS) and IR (LPMA) spectrometers analyze direct light from either the whole solar disk (DOAS), or from its inner core (LPMA). Thus, the analyzed sunlight traversed almost the same atmospheric air masses (except for the slightly different effective FOV of both spectrometers). The measurements are performed during balloon ascent or descent and in solar occultation geometry, with moderate spectral resolution in the UV/visible (UV: FWHM = 0.5 nm, visible: FWHM = 1.5 nm) and high spectral resolution in the IR (unapodized resolution 0.02 cm^{-1}).

From the direct sunlight spectra, slant column amounts of the targeted atmospheric absorbers are inferred, using either the DOAS approach in the UV/visible (Platt and Stutz, 2006), or the conventional least squares spectral retrieval technique in dedicated micro-windows, in the near-IR. Upon trace gas retrieval the measured slant column amounts or absorptions of the measured species are inverted into trace gas profiles by applying the truncated Singular Value Decomposition (SVD) or the Maximum A Posteriori (MAP) inversion technique (Rodgers, 2000). For the profile inversion of reactive species (e.g. NO_2 and BrO), a correction based on photochemical modelling is included (e.g. Butz et al., 2006).

The novel mini-DOAS deployed on the LPMA/DOAS gondola (and during several MIPAS-B2 flights), analyzes limb radiances perpendicular to the sun's azimuth direction. From the received sunlight, profiles of the limb scattered radiance of O_3, NO_2 and BrO (and possibly in future also of OClO, IO, OIO and CH_2O) are analyzed (Weidner, 2005). Prior to the balloon flights, the instrument is absolutely calibrated by an Ulbricht sphere. The primary results are skylight radiances and, after applying the DOAS method, trace gas slant column densities (SCD) along the line-of-sight. Radiative Transfer (RT) calculations are used to (a) simulate the measured quantities and (b) infer vertical profiles of O_3, NO_2, and BrO by applying the Maximum A Posteriori (MAP) inversion technique (Rodgers (2000)). This allows for a stringent validation of the applied RT codes (e.g. TRACY or SCIATRAN).

2.2. RT Modelling :

For the direct sun observations RT calculations are performed by modelling the path of the light from the sun to the balloon borne detector for each line-of-sight in a spherical, refractive atmosphere. The obtained weighting functions are given by the ratio of the slant to the vertical light paths through each atmospheric layer (Box Air Mass Factors, BoxAMF). It has to be pointed out that for the direct sun observations the BoxAMF do not depend on any ambient parameters except for pressure and temperature through the refractive index. For skylight limb (mini-DOAS) observations, the 3-D Monte Carlo Radiative Transfer Model (MC RTM) 'TRACY' is used, which was developed at the IUP Heidelberg (von Friedeburg, 2004). The RTM solves the radiative transfer equation by backward Monte Carlo simulations in a fully spherical 3-dimensional and refractive atmosphere. It supports an arbitrary spatial discretization and takes into account multiple scattering with arbitrary phase functions. As input, TRACY uses atmospheric profiles of temperature, pressure, aerosol extinction and ozone concentration. The outputs are wavelength dependent limb and nadir radiances, slant column densities along the line-of-sight of the trace gases of interest and the corresponding BoxAMFs.

2.3 Trajectory modelling:
Balloon-borne measurements are inherently restricted by different constraints, limiting their flexibility in satellite validation. Therefore, trajectory modelling was also included into the validation, in order to find best coincidences between air masses probed by the balloon-borne instruments and Envisat/SCIAMACHY observations. The trajectory model uses the operational analyses and forecasts of the European Centre for Medium Range Weather Forecasts (ECMWF) - or a combination of both - given every 6 h on a 2.5° x 2.5° latitude/longitude grid. The ECMWF data are interpolated to 25 user-defined isentropic levels extending from the surface up to 1600 K. The internal time step for integrating the path of the air masses is 10 min and the diabatic and climatological heating rates are based on Newtonian cooling. The results (trajectory points) are stored for each hour (e.g. Langematz (1987)).
Backward and forward trajectories are started at the balloon measurement locations, which depend on the individual measurement technique. For the LPMA / DOAS remote-sensing payload, the start and end points are calculated from knowledge of the balloon flight trajectory and the known observation geometry given by the line-of-sight for each measurement. For post-flight analysis, forward and backward trajectories are calculated for up to 10 days, but for balloon flight planning purposes the time range is limited by the available ECMWF forecasts (analyses are available up to 12:00 UT of the day before, forecasts for every 6 h up to 72 h).
The actual geolocations of SCIAMACHY observations are taken from the SCIAMACHY Operational Support Team (SOST) on their website (*http://atmos.af.op.dlr.de/projects/scops*). Here, the overpass time, the geolocation and detailed measurement specifications (e.g. swath, measurement duration, ground pixel size) are

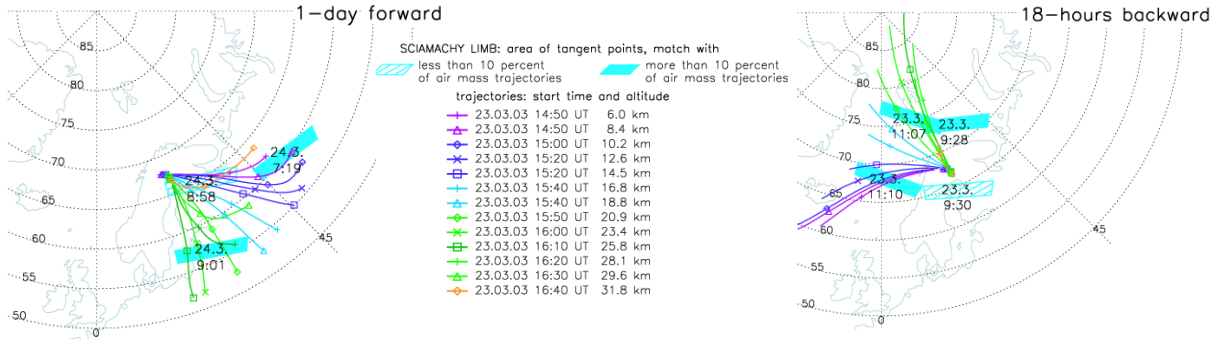

Fig. 1: Air mass trajectories modelled 18 hours backward (left panel) and 24 hours forward (right panel) in time for the balloon ascent measurements of the LPMA/DOAS payload at Kiruna on March 23, 2003. The trajectories are color-coded according to their starting altitude as indicated in the legend. A symbol is plotted every 12 hour interval. The areas covered by the tangent points of SCIAMACHY limb observations are projected onto the Earth's surface and illustrated as blue rectangles. Filled rectangles correspond to SCIAMACHY limb observations for which more than 10% of the calculated air masses are coincident with the LPMA/DOAS measurements. The shaded rectangles represent SCIAMACHY limb observations for which less than 10% of the calculated air masses are coincident with the LPMA/DOAS measurements. The time and date of the satellite measurements is given next to the rectangles (courtesy of FU-Berlin).

downloaded for the SCIAMACHY limb and for the SCIAMACHY nadir mode for each Envisat orbit. For the air mass trajectory-based matching technique only the area covered by tangent points (light blue areas in Fig. 1) of SCIAMACHY limb observation is considered in more detail. This information is used to find satellite measurement points along individual air mass trajectories, for which the spatial and temporal mismatch is as small as possible. The match criterion is chosen based on the experience of the ozone Match experiment e.g. Gathen et al. (1995): a time mismatch between the satellite observation and the air mass trajectory started at the balloon observation of < ± 1 h and an area mismatch of < ± 500 km. If SCIAMACHY observations do not fulfil these criteria, the distance criterion is extended up to 1000 km.

2.4 Photochemical modelling:
As outlined above, the use of a validated 3-D CTM photochemical model is necessary when different measurements of stratospheric radicals are compared and validated. Fig. 2 demonstrates why the model has to be used to compare SCIAMACHY BrO (or NO_2) limb measurements (left panel) with LPMA / DOAS balloon ascent and occultation observations (right panel). In both panels, the line-of-sights are indicated by thin black lines. In addition, the thick black line in the right panel represents the balloon trajectory. Here the observations are super-imposed by a photochemical simulation of stratospheric BrO from the SLIMCAT 3-D CTM Chipperfield (1999) for March 23, 2003.
SLIMCAT is a 3-D off-line CTM with detailed treatment of the stratospheric photochemistry. The model temperatures and horizontal winds are specified from ECMWF analyses. The vertical transport in the stratosphere is diagnosed from radiative heating rates. In the stratosphere the model uses an isentropic coordinate

extended down to the surface using hybrid sigma-theta levels (M.P. Chipperfield, private communication). The troposphere is assumed to be well-mixed.
The CTM is integrated with a horizontal resolution of 7.5° x 7.5° and 24 levels extending from the surface to about 55 km. The model is forced using ECMWF analyses and the simulation starts on 1 January 1977. The model halogen loading is specified from observed tropospheric CH_3Br and halon loadings WMO (2003). In addition, an extra 4 pptv bromine is modelled in a tracer to represent bromine-containing very short-lived substances (VSLS) and 1 pptv is assumed to be transported to the stratosphere as Br_y (Feng et al., 2006). Output is saved at 00:00 UT every 2 days, interpolated to the location of the balloon flights. A 1-D column model is then used to reconstruct the diurnal cycle for comparison with the observations.

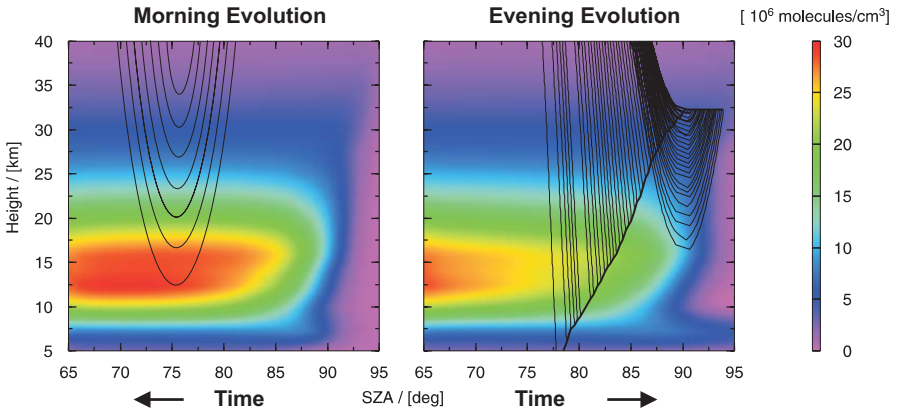

Fig. 2: Color-coded model concentration field of BrO as a function of height and SZA, for the DOAS balloon flight on 23 March 2003 at Kiruna (67.9°N, 22.1°E). Left and right panels show the morning and evening evolution of BrO, respectively. The black lines in the left panel represent the line-of-sight of a SCIAMACHY limb scan. In the right panel the observation geometry of the DOAS measurements is shown for every twentieth spectrum measured during ascent and every tenth spectrum during solar occultation. The thick black line represents the trajectory of the balloon and the thin black lines indicate the optical path from the Sun to the balloon instrument for measurements during ascent and solar occultation. Note that in the real atmosphere the lines-of-sight are close to being straight lines, but the projection of the Earth's curvature on a straight x-axis causes the lines-of-sight to appear curved in the presentation. Figure adopted from Dorf et al. (2006).

The vertical 1-D column model simulates stratospheric photochemistry on forward and backward air mass trajectories (described above) with the aim to find best guess profiles for the satellite observations based on the different validation balloon measurements. The stratospheric photochemistry is modelled on 20 potential temperature (Θ) levels between Θ =323 K and Θ = 1520 K. The 1-D column model is initialized, at each height level, at 00:00 UT with 3-D CTM SLIMCAT model results at an adjacent 48 hour model time step at the balloon launch site.
The model is constrained to follow the evolution of the SZA time-line, which is taken from the air mass trajectory calculations. In satellite validation, these measures guarantee that the photochemical evolution of the modeled air mass is a good approximation of the true evolution between initialization of the model, the satellite measurement and balloon-borne observation. For simplicity a single representative SZA time-line is chosen for all Θ levels and the model is run with fixed pressure and temperature for each Θ level taken from the meteorological support data of the balloon flight.
Furthermore, each observation conducted by the remote sensing instruments SCIAMACHY and LPMA/DOAS is a composite of changing photochemical conditions (due to changing SZA) along the line-of-sight (Fig. 2).
Photochemical-weighting factors are calculated to scale balloon observations to the photochemical conditions of the satellite measurements. In the case of LPMA / DOAS measurements the scaling is implicitly considered by the profile inversion algorithm as described by Butz et al., (2006). A flow diagram of the overall validation procedure is given in Fig. 3.

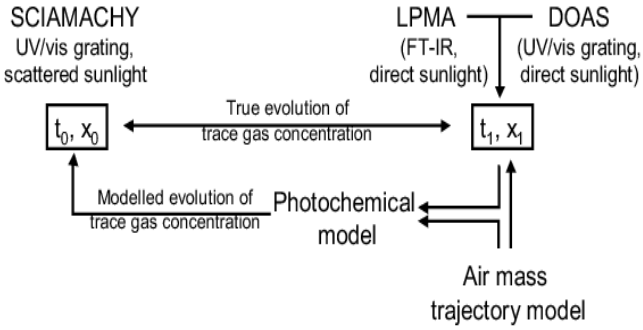

Fig. 3: Schematic drawing of the presented validation strategy. SCIAMACHY observations are conducted at time t_0 and location x_0. Prior to the balloon flight dedicated to SCIAMACHY validation, an air mass trajectory model is used to optimize the time t_1 and location x_1 of the LPMA / DOAS balloon borne observations, e.g. by optimizing the launch time of the balloon. After the balloon flight, the trajectory model calculates the air mass history in order to identify satellite measurements, which actually sampled the same air masses as the balloon-borne instruments. For the validation of photochemically active trace species, the illumination history of the coincident air masses is fed into a photochemical model to reproduce the evolution of the considered trace gases between satellite and balloon-borne observations as realistically as possible and to infer appropriate scaling factors. Figure adopted from Butz et al. (2006).

3. PPRODUCTS & RESULTS

3.1 Validation of level 1 products:

In a first level 1 validation study, absolutely calibrated solar irradiance spectra are measured, at around 33 km balloon float altitude, with a moderate resolution in the UV/visible spectral range (in the UV from 316.7 to 418 nm and in the visible from 400 to 652 nm at a full width half maximum resolution of 0.55 nm and 1.48 nm, respectively) After accounting for atmospheric extinction due to Rayleigh scattering and gaseous absorption (O_3 and NO_2), the measured solar spectra are compared with previous observations. Our solar irradiance spectrum perfectly agrees within +0.03% with the re-calibrated Kurucz et al. (1984) solar spectrum (Fontenla et al., 1999 - called MODTRAN 3.7) in the visible spectral range (415 to 650 nm), but it is +2.1% larger in the 370 to 415 nm wavelength interval, and −4% smaller in the UV-A spectral range 316.7 to 370 nm, when the Kurucz spectrum is convolved to the spectral resolution of our instrument. Similar comparisons of the SOLSPEC (Thuillier et al., 1997, 1998a, b) and SORCE/SIM (Harder et al., 2000) solar spectra with MODTRAN 3.7 confirm our findings with the values being -0.5%, +2%, and -1.4% for SOLSPEC, and -0.33%, -0.47%, and -6.2% for SORCE/SIM, respectively. Comparison of the SCIAMACHY solar spectrum from channels 1 to 4 with MODTRAN 3.7 indicates an agreement within −0.4% in the visible spectral range from 415 to 585 nm, - 1.6% between 370 and 415 nm, and - 5.7% within the 325 to 370 nm wavelength interval. This is in agreement with the results of the other sensors. In agreement with findings of Skupin et al. (2002), our study emphasizes that the past ESA SCIAMACHY level 1 calibration is systematically +15% larger in the considered wavelength intervals when compared to all available other solar irradiance measurements. Agreement of the SCIAMACHY data with the validation data set can be significantly improved by using the IUP-Bremen re-calibration.

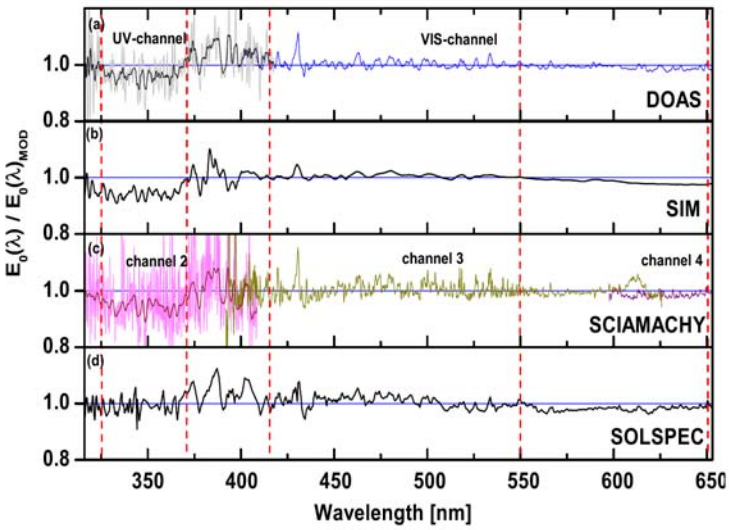

Fig. 5: Ratio of solar irradiance spectra ($E_o(\lambda)/E_o(\lambda)_{MOD}$) referenced to the solar spectrum of Kurucz et al. (1984) with recent updates of Fontenla et al. (1999) (MODTRAN 3.7) with (a) the present measurement, (b) SORCE/SIM (Harder et al., 2000), (c) SCIAMACHY in channel 1, 2, 3, and 4 using the revised IUP-Bremen calibration, and (d) SOLSPEC (Thuillier et al., 1997, 1998b). For the comparison, the MODTRAN 3.7 solar spectrum is convolved to the spectral resolution of the individual instruments, using a least squares fitted Gaussian instrument function as provided by the WINDOAS fitting tool. For the balloon and SCIAMACHY measurements, an additional 1.5 nm wide Gaussian smoothing is applied to the ratioed spectra (light grey and pink lines) for $\lambda < 418$ nm in order to illustrate baseline effects (filled black and pink lines, respectively). Figure adopted from Gurlit et al. (2005).

3.2 Validation of RT Models:

In a second study, the limb radiances and trace gas absorptions measured by mini-DOAS are compared with RT modelling using TRACY and SCIATRAN. Generally, reasonable agreement is found between (a) measured and RT calculated limb radiances (see Fig. 5), and (b) inferred mini-DOAS limb O_3, NO_2, BrO and correlative profile measurements, when properly accounting for all relevant atmospheric parameters (temperature, pressure, aerosol extinction, and major absorbing trace gases). Additionally, scanning limb observations allow for time-resolved trace-gas measurements of radicals as a function of the Solar Zenith Angle (SZA) and the validation of the applied photochemical models (see section 2.3) and therein used photolysis rates. For further discussions of the results obtained from the mini-DOAS measurements see Weidner et al. (2005) and Weidner (2005).

3.3 Validation of level 2 products:

We report on 4 LPMA / DOAS validation balloon flights performed since 2003. Three were conducted from ESRANGE, Kiruna, Sweden and one from Aire sur l'Adour in southern France (see Table 1). The analysis of a fifth balloon flight from Teresina, Brazil, in June 2005 is currently in preparation. For each balloon flight a satellite coincident measurement is identified in the morning before and after the balloon flight using the trajectory matching technique described above (Fig.1). In the following we refer to these coincidences as backward and forward coincidences. If trace gas profiles inferred from balloon ascent and solar occultation are available, the satellite coincidences are identified separately. For each balloon flight table 1 provides information

on the measurement site, the geophysical condition, the SZA range covered by the balloon-borne observations, the available data sets and some details on the selected SCIAMACHY limb scans.

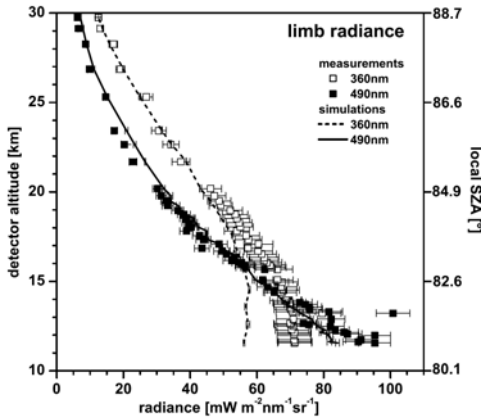

Fig. 5: Comparison of measured and TRACY modelled limb radiance at 360 nm (open squares and dashed line) and 490 nm (filled squares and full line, respectively) for an azimuth angle of 90° and an elevation angle of +0.5° during balloon ascent at Kiruna on March 23, 2003. Also denoted is the Solar Zenith Angle (SZA) at the balloon position. Figure adopted from Weidner et al. (2005).

3.3.1 O_3 validation:

Figure 6 shows an illustrative example for the agreement between SCIAMACHY O_3 profiles inferred by the IUP-Bremen retrieval and the coinciding LPMA / DOAS balloon-borne observations. Figure 7 summarizes all considered data by showing the relative differences between balloon and satellite-borne observations of O_3. In most cases SCIAMACHY limb O_3 profiles agree to within ±20% with the validation data set in the 20 km to 30 km altitude range. The relative deviations show a systematic underestimation of the balloon-borne by the satellite-borne profiles at 24 km to 28 km altitude. This finding is similar to conclusions of Brinksma et al. (2005), where a zigzag shape of the deviations between a validation data set (Lidar, SAGE II) and the IUP-Bremen O_3 retrieval is observed, indicating that O_3 concentrations at 27 km inferred from SCIAMACHY limb are too low. Albeit different corrections for tangent height errors are already included in the SCIAMACHY retrievals, there might be a remaining small tangent height error causing the observed deviations. Below 20 km SCIAMACHY O_3 profiles underestimate the balloon-borne data in most cases and cannot reproduce the frequently highly filamented O_3 profiles especially observed at high-latitudes during winter. Deviations in the lower stratosphere might be due to the lower sensitivity of the satellite retrieval or unaccounted horizontal trace gas variations.

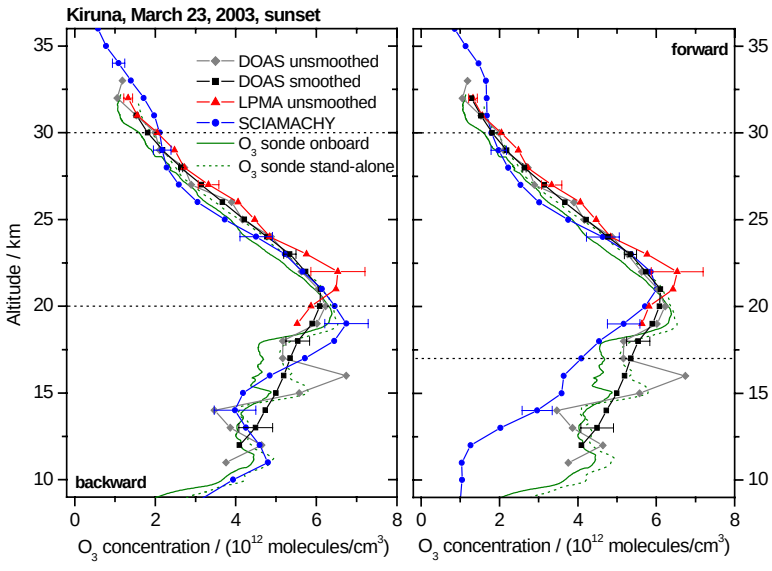

Fig. 6: Comparison of O_3 profiles inferred from SCIAMACHY limb observations with correlative balloon borne measurements. The observations are conducted during sunset at Kiruna on March 23, 2003. The left and right panel corresponds to a backward and a forward coincidence, respectively. Satellite data inferred by IUP-Bremen are shown as blue circles. Appropriately smoothed DOAS data are plotted as black boxes, LPMA data as red triangles. The grey diamonds represent DOAS profiles at full altitude resolution without smoothing. O_3 profiles measured by an electrochemical cell aboard the gondola during balloon ascent are shown as green line. The dashed green line corresponds to measurements of a stand-alone in-situ sonde launched from the ground station shortly after balloon launch. The altitude range between the horizontal dotted lines represents the range where coincident air masses are found. For better visibility, only selected error bars are shown. Figure adopted from Butz et al. (2006).

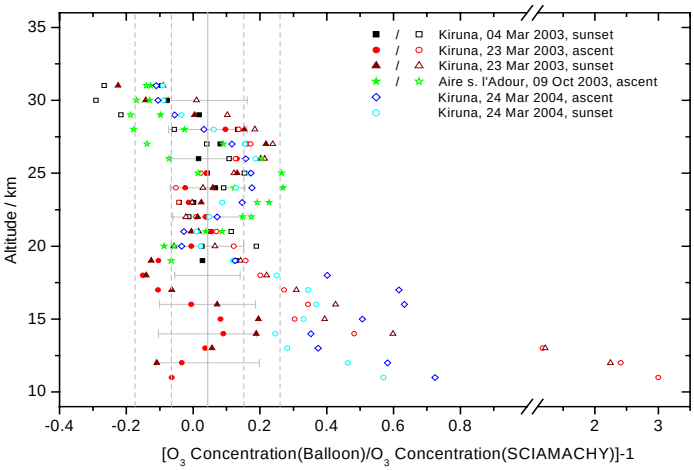

Fig. 7: Relative deviations between SCIAMACHY and LPMA / DOAS measurements of O_3. Filled and open symbols correspond to backward and forward coincidences, respectively. Observation sites and conditions are indicated in the legend. The mean deviation of all coincident data in the 20 –31 km altitude range is 4.3% (solid grey line) with 10.8% standard deviation (dashed grey lines for 1-σ and 2-σ). The grey error bars indicate the mean combined errors of the satellite and balloon borne observations. Note the broken abscissa. Figure adopted from Butz et al. (2006).

3.3.2 NO_2 validation:

Figure 8 shows an illustrative comparison between SCIAMACHY NO_2 profiles inferred by the IUP-Bremen, Harvard, and IUP-Heidelberg retrievals and the coinciding LPMA / DOAS balloon-borne observations. The relative deviations between the satellite and balloon-borne observations are shown in Fig. 9. In the 20 km to 30 km altitude range the agreement between the balloon-borne NO_2 profiles and the satellite observations is on the order of ±20% and most often well represented by the combined error bars. The NO_2 profile inferred by the Harvard algorithm for the backward coincidence in the left panel of Fig. 8 is offset by +2 km to +3 km since no correction of tangent height errors is performed in this particular case. Clearly, such a correction would improve the agreement with the validation data as can be seen from the IUP-Bremen and IUP-Heidelberg profiles and from the forward coincidence. Below 20 km, SCIAMACHY tends to underestimate the balloon-borne data, which is clearly observable, although error bars are large. NO_2 profiles retrieved by the IUP-Bremen, IUP-Heidelberg and Harvard algorithms exhibit sizeable discrepancies below 20 km. This indicates that for low altitudes the SCIAMACHY retrieval might depend on the actual parameters, e.g. a priori information, used. The latter finding is supported by the characteristics of the corresponding averaging kernels (not shown).

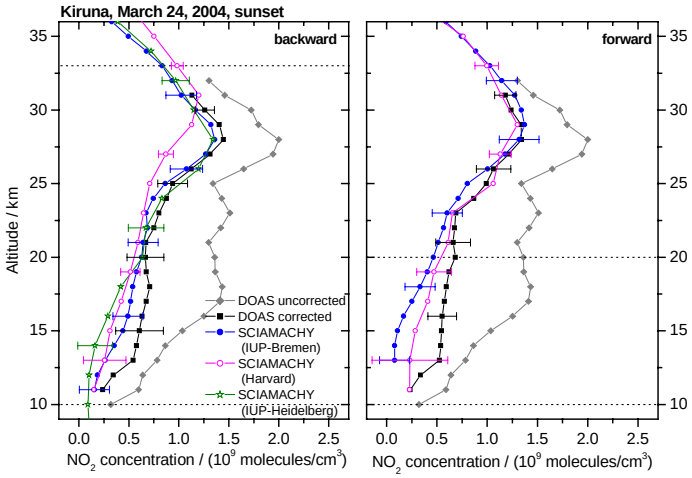

Fig. 8: Comparison of NO_2 profiles inferred from SCIAMACHY limb observations with correlative balloon-borne measurements. The observations were conducted at Kiruna on March 24, 2004, during sunset. The left and right panel corresponds to a backward and a forward coincidence, respectively. Satellite data inferred by IUP-Bremen are shown as blue circles, by Harvard as magenta open circles and by IUP-Heidelberg as green open stars. Appropriately smoothed DOAS data are plotted as black boxes. The grey diamonds represent DOAS profiles at full altitude resolution without smoothing. The altitude range between the horizontal dotted lines represents the range where coincident air masses are found. For better visibility, only selected error bars are shown. Figure adopted from Butz et al. (2006).

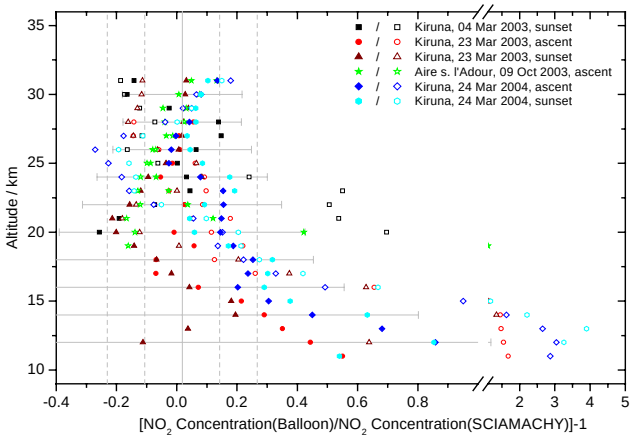

Fig. 9: Relative deviations between SCIAMACHY (IUP-Bremen) and LPMA / DOAS measurements of NO_2. Filled and open symbols correspond to backward and forward coincidences, respectively. Observation sites and conditions are indicated in the legend. SCIAMACHY data corresponding to the backward coincidence on March 4, 2003, at Kiruna are shifted by −2 km. The mean deviation of all coincident data in the 20 km–31 km altitude range is 1.8% (solid grey line) with 12.4% standard deviation (dashed grey lines for 1-σ and 2-σ). The grey error bars indicate the mean combined errors of the satellite and balloon borne observations. Note the broken abscissa. Figure adopted from Butz et al. (2006).

3.3.3 BrO validation:

Figure 10 shows an example of a comparison of BrO profiles measured by the DOAS balloon instrument and SCIAMACHY. Stratospheric BrO abundances measured from 3 different balloon sensors (DOAS, SAOZ, Triple) are compared in Dorf et al. (2006) with first retrieval exercises of SCIAMACHY BrO limb profiling from the Harvard group. Total Br_y = (20.1 ± 2.8) pptv, obtained from DOAS BrO observations at mid-latitudes in 2003, serves as an upper limit of the comparison. The good agreement of balloon trace gas measurements with the SLIMCAT model indicates that vertical transport is considered correctly and was not a major source of error. Within the given range of errors of the different measurement techniques, most of the balloon observations agree with model BrO. Initial BrO profiles available from the Harvard-Smithsonian SCIAMACHY retrieval agree on average to around 20 % with the photochemically corrected balloon observations (SAOZ and DOAS). In general, the satellite measurements show systematically higher values below 25 km and a change in profile shape above about 25 km.

The presented set of BrO balloon profiles is meant to be representative and, according to the trajectory calculations, the most suitable set of SCIAMACHY BrO validation profiles and it is thus recommended for future SCIAMACHY limb BrO retrieval exercises.

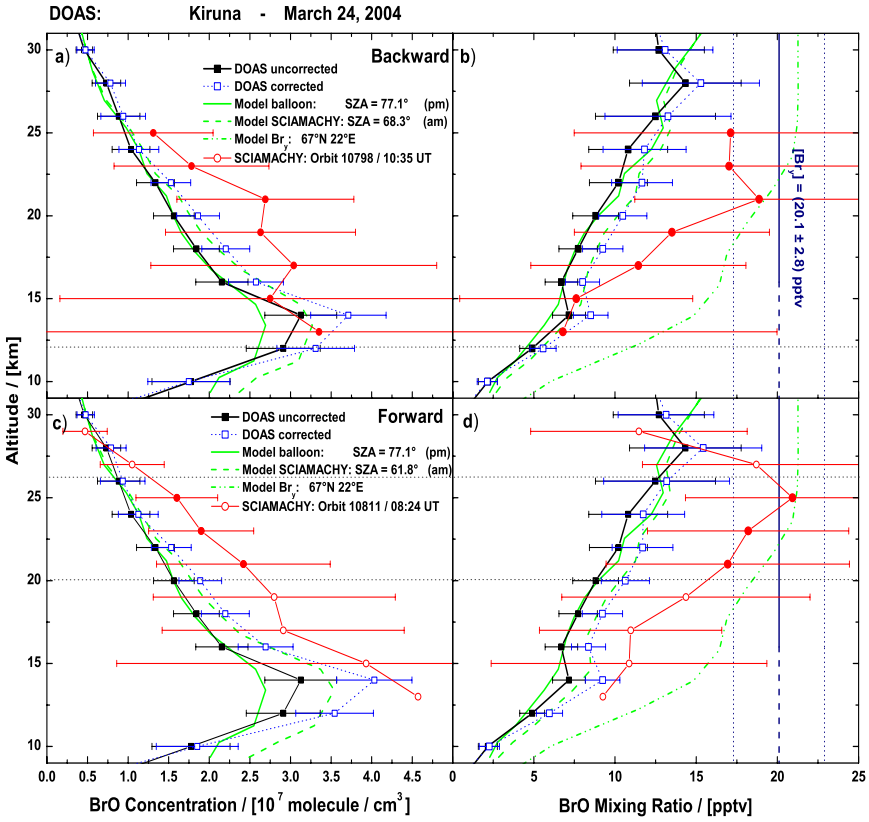

Fig. 10: Comparison of a BrO profile measured by DOAS during balloon ascent on March 24, 2004 at Kiruna with model calculations and SCIAMACHY limb retrievals. Black squares represent the photochemically-uncorrected balloon measurement and blue squares the balloon profile photochemically corrected to the SZA of the SCIAMACHY measurement. Corresponding model profiles at the SZA of the balloon and satellite observations are shown as solid and dashed green lines respectively. Total inorganic Br_y volume mixing ratios as used in the model (green dash-dotted line) and as retrieved by DOAS measurements (vertical dark blue lines, see text for details) are also indicated. SCIAMACHY measurements are shown as solid red circles in the altitude range for the match, which is indicated as thin dotted horizontal lines, and as open red circles outside this range. Panels (a) and (b) show calculations for the 'best' backward match and Panels (c) and (d) for the 'best' forward match. Figure adopted from Dorf et al. (2006).

4. SUMMARY & CONCLUSION

Level 1 and 2 products of Envsiat / SCIAMACHY have been validated by so far 5 deployments of the LPMA / DOAS payload at high, mid and low-latitudes since 2003. Overall reasonable agreement is found for the level 1 products solar irradiance and limb radiance (< ± 5%), after the previous SCIAMACHY spectral irradiance calibration was updated with supporting results from the present validation observations. For validation of level 2, not yet operational, products (O_3, NO_2 and BrO) inferred by 3 scientific groups (IUP-HD, IUP-Bremen and Havard-Smithsonian), variable good agreement is obtained. The methods and results presented here are discussed in detail in Gurlit et al. (2005), Weidner et al. (2005), Dorf et al. (2006) and Butz et al. (2006). They are also of value for the validation of other existing satellite measurements of BrO, NO_2 and O_3 (e.g. OMI) or satellite instruments, that intend to measure these trace gases in the future (e.g. GOME-2). Our future validation activities will particularly concentrate (1) on the level 2 SCIAMACHY products OClO (at high-latitudes) and O_3, NO_2, BrO, IO, OIO, … obtained at low latitudes and (2) the validation of complementary data products from the ENVISAT MIPAS and GOMOS instruments.

For future validation studies including operational products from ESA, digital copies of all balloon-borne DOAS related products for all validation flights, can be obtained from the NILU data server (http://www.nilu.no), upon signing the data protocol of the ESA sponsored Envisat validation activities. DOAS data is also available on http://www.iup.uni-heidelberg.de/institut/forschung/groups/atmosphere/stratosphere/ .

Acknowledgement: Support of the project by Bundesministerium für Bildung und Forschung (BMBF) through grants 50EE0017, and 50EE0019, the Deutsche Forschungsgemeinschaft (DFG) Pf 384/3-1 and 384/5-1, and European Union (EU) through grants EVK2-CT-2000-00059 (QUILT) GOCE-CT-2004-505337 (ACCENT), EVK2-CT-2001-00111 (HIBISCUS) and 505390-GOCE-CT-2004 (SCOUT-O3) is highly acknowledged. Additional support came through the European Space Agency by the ESABC project (AO 146, AO 465, AO 629 and AO 694). We thank the technical team of LPMA (Y. Té, P. Jeseck, and V. Ferreira) for the assistance given to perform successfully the balloon flights. We are also grateful to the CNES teams 'equippe nacelles pointées' and the balloon launching team from Aire-sur-l'Adour / France without which the successful launch of the balloons would have been impossible. We also acknowledge the support given by Physikalisch-Technische Bundesanstalt (PTB) Braunschweig (A. Höpe und P. Sperfeld) in the commissioning of the absolute radiometric standards.

References:

1. Bovensmann, H.: SCIAMACHY: Mission Objectives and Measurement Modes, J. Atmos. Sci., 56, 127 - 150, 1999.
2. Brinksma, E. J., Bracher, A., Lolkema, D. E., Segers, A. J., Boyd, I. S., Bramstedt, K., Claude, H., Godin-Beekmann, S., Hansen, G., Kopp, G., Leblanc, T., McDermid, I. S., Meijer, Y. J., Nakane, H., Parrish, A., von Savigny, C., Strebel, K., Swart, D. P. J., Taha, G., and Piters, A. J. M.: Geophysical validation of SCIAMACHY Limb Ozone Profiles, Atmos. Chem. Phys., 6, 197 - 209, 2006.
3. Butz, A., H. Bösch, C. Camy-Peyret, M. Chipperfield, M. Dorf, G. Dufour, K. Grunow, P. Jeseck, S. Kühl, S. Payan, I. Pepin, J. Pukite, A. Rozanov, C. von Savigny, C. Sioris, F. Weidner, K. Pfeilsticker, Inter-comparison of stratospheric O_3 and NO_2 abundances retrieved from balloon-borne direct sun observations and Envisat/SCIAMACHY limb measurements, Atmos. Chem. Phys., 6, 1293 -1314, 2006.
4. Camy-Peyret, C.: Balloon-borne Fourier transform spectroscopy for measurements of atmospheric trace gases, Spectrochim. Acta, 51A, 1143 - 1152, 1995.
5. Canty, T., R.S. Salawitch, J.B. Renard, E.D. Reviere, K. Pfeilsticker, M. Dorf. R. Fitzenberger, H. Bösch, R.M. Stimpfle, D.M. Wilmouth, J.G. Anderson, E.C. Richard, D.W. Fahey, R.S. Gao, and T.P. Bui, Analysis of BrO, ClO, and nighttime OClO in the arctic winter stratosphere, J. Geophys. Res., 110, D01301, doi:10.1029/2004JD005035, 2005.
6. Chipperfield, M. P.: Multiannual simulations with a three-dimensional chemical transport model, J. Geophys. Res., 104, 1781 - 1805, 1999.
7. Dorf, M., H. Bösch, A. Butz, C. Camy-Peyret, M. P. Chipperfield, A. Engel, F. Goutail, K. Grunow, F. Hendrick, S. Hrechanyy, B. Naujokat, J.-P. Pommereau, M. Van Roozendael, C. Sioris, F. Stroh, F. Weidner, and K. Pfeilsticker, Balloon-borne stratospheric BrO measurements: Comparison with Envisat / SCIAMACHY BrO limb profiles, ACP (revised) 2006.
8. Dufour, G., Payan, S., Lefévre, F., Eremenko, M., Butz, A., Jeseck, P., Té, Y., Pfeilsticker, K., and Camy-Peyret, C.: 4-D comparison method to study the NO_y partitioning in summer polar stratosphere – Influence of aerosol burden, Atmos. Chem. Phys., 5, 919 - 926, 2005.
9. Feng, W., M.P. Chipperfield , M. Dorf and K. Pfeilsticker, Mid-latitude Ozone Changes: Studies with a 3-D CTM Forced by ERA-40 Analyses, ACPD (accepted), 2006.
10. Ferlemann, F., Camy-Peyret, C., Fitzenberger, R., Harder, H., Hawat, T., Osterkamp, H., Schneider, M., Perner, D., Platt, U., Vradelis, P., and Pfeilsticker, K.: Stratospheric {BrO} profiles measured at different latitudes and seasons: Instrument description, spectral analysis and profile retrieval, Geophys. Res. Lett., 25, 3847 - 3850, 1998.
11. Ferlemann, F., Bauer, N., Fitzenberger, R., Harder, H., Osterkamp, H., Perner, D., Platt, U., Scheider, M., Vradelis, P., and Pfeilsticker, K.: Differential optical absorption spectroscopy instrument for stratospheric balloon-borne trace gas studies, Appl. Opt., 39, 2377 - 2386, 2000.
12. Fontenla, J., White, O. R., Fox, P. A., Avrett, E. H., and Kurucz, R. L.: Calculation of solar irradiances, I. Synthesis of the solar spectrum, Astrophys. J., 518, 480 - 500, 1999.
13. von Friedeburg, C., Derivation of Trace Gas Information combining Differential Optical Absorption Spectroscopy with Radiative Transfer Modelling, Dissertation, Universität Heidelberg, 2004, http://www.ub.uni-heidelberg.de/archiv/3758
14. Frieler, K., M. Rex, R.J. Salawitch, T. Canty, M. Streibel, R.M Stimpfle, K. Pfeilsticker, M. Dorf, D.K. Weisenstein, S. Godin-Beekmann, P. von der Gathen, Towards a better quantitative understanding of polar stratospheric ozone loss, Geophys. Res. Lett., (in press), 2005.

15. von der Gathen, P., Rex, M., Harris, N., Lucic, D., Knudsen, B., Braathen, G., Backer, H. D., Fabian, R., Fast, H., Gil, M., Kyr, E., Mikkelsen, I., Rummukainen, M., Sthelin, J., and Varotsos, C.: Observational evidence for chemical ozone depletion over the Arctic in winter 1991 - 92, Nature, 375, 131 - 134, 1995.
16. Gurlit, W., H. Bösch, H. Bovensmann, J. P. Burrows, A. Butz, C. Camy-Peyret, M. Dorf, K. Gerilowski, A. Lindner, S. Noel, U. Platt, F. Weidner, and K. Pfeilsticker, The UV-A and visible solar irradiance spectrum: Inter-comparison of absolutely calibrated, spectrally medium resolved solar irradiance spectra from balloon-, and satellite-borne measurements, Atmos. Chem. Phys., 5, 1879 - 1890, 2005.
17. Harder, J., G. Lawrence, G. Rottman, and T. Woods, The Spectral Irradiance Monitor (SIM) for the SORCE Mission, Proc. SPIE, 4135, pp. 204 - 214, see: http://lasp.colorado.edu/sorce/ presentation/SORCE Brochure 10 25 FINAL.pdf, 2000.
18. Hawat, T. M., Camy-Peyret, C., and Torguet, R. J.: Suntracker for atmospheric remote sensing, SPIE Optical Engineering, May 1998, 37(05), 1633 - 1642, 1998.
19. Kurucz, R. L., Furenhild, I., Brault, J., and Testermann, L.: Solar flux atlas from 296 to 1300 nm, National Solar Observatory Atlas No. 1, June 1984, (ftp://ftp.noao.edu/fts/fluxatl), 1984.
20. Langematz, U., Labitzke, K. and Reimer, E.: Synoptic analysis and trajectories during the MAP/GLOBUS campaign 1983, Planetary and Space Science, 35, 525 - 538, 1987.
21. Platt, U. and J. Stutz, Differential Optical Absorption Spectroscopy, Principle and Applications, Springer Verlag, Heidelberg, ISBN 3-340-21193-4, 2006.
22. Rodgers, C. D., Inverse Methods For Atmospheric Sounding, World Scientific, Singapure, New Jersey, London, Hong Kong, 2000.
23. Sierk, B., Richer, A., Rozanov, A., von Savigny, C, Schmoltner, A. M., Buchwitz, M., Bovensmann, H., and Burrows, J. P.: Retrieval and monitoring of atmospheric trace gas concentrations in nadir and limb geometry using the space-borne SCIAMACHY instrument, Environmental Monitoring and Assessment (in press) 2006.
24. Sioris C. E., C. S. Haley, C. A. McLinden, C. von Savigny, I. C. McDade, W. F. J. Evans, J. C. McConnell, N. D. Lloyd, E. J. Llewellyn, D. Murtagh, U. Frisk, T. P. Kurosu, K. V. Chance, K. Pfeilsticker, H. Bösch, and F. Weidner, Stratospheric profiles of nitrogen dioxide observed by OSIRIS on the Odin satellite, J. Geophys. Res., 108, NO. D7, 4215, doi: 10.1029/2002JD002672, 2003.
25. Sioris, C.E., L. J. Kovalenko, C. A. McLinden, R. J. Salawitch, M. Van Roozendael, F. Goutail, M. Dorf, K. Pfeilsticker, K. Chance, C. von Savigny, X. Liu, T. P. Kurosu, J.-P. Pommereau, H. Bösch, and J. Frerick, Latitudinal and vertical distribution of bromine monoxide in the lower stratosphere from SCIAMACHY limb scattering measurements, J. Geophys. Res., (in press) 2006.
26. Skupin, J., Nöel, S., Wuttke, M. W., Bovensmann, H., and Burrows, J. P.: Calibration of SCIAMACHY in-flight measured irradiances and radiances-first results of level 1 validation, Proc. of the Envisat Validation Workshop (SP-531), ESA Publications Division, 2002.
27. Thuillier, G., Hersé, M., Simon, P. C., Labs, D., Mandel, H., and Gillotay, D.: Observation of the UV solar irradiance between 200 and 350 nm during the ATLAS-1 mission by the SOLSPEC spectrometer, Sol. Phys., 171, 283 - 302, 1997.
28. Thuillier, G., Hersé, M., Simon, P. C., Labs, D., Mandel, H., Gillotay, D., and Foujols, T.: The visible solar spectral irradiance from 350 to 850 nm as measured by the SOLSPEC spectrometer during the ATLAS-1 mission, Sol. Phys., 177, 41 - 61, 1998a.
29. Thuillier, G., Hersé, M., Simon, P. C., Labs, D., Mandel, H., and Gillotay, D.: Solar radiometry and solar spectral irradiance: Observation of the solar spectral irradiance from 200 nm to 870 nm during the ATLAS 1 and ATLAS 2 missions by the SOLSPEC spectrometer, Metrologia, 35, 689 - 697, 1998b.
30. Weidner, F., Development and Application of a Versatile Balloon-Borne DOAS Spectrometer for Skylight Radiance and Atmospheric Trace Gas Profile Measurements, Dissertation, Universität Heidelberg, 2005, http://www.ub.uni-heidelberg.de/archiv/5503
31. Weidner, F., H. Bösch, H. Bovensmann, J. P. Burrows, A. Butz, C. Camy-Peyret, M. Dorf, K. Gerilowski, W. Gurlit, U. Platt, C. von Friedeburg, T. Wagner, and K. Pfeilsticker, Balloon-borne Limb profiling of UV/vis skylight radiances, O_3, NO_2, and BrO: Technical set-up and validation of the method, Atmos. Chem. Phys., 5, 1409 - 422, 2005.
32. WMO: Scientific Assessment of Ozone depletion: 2002, World Meteorological Organization Global Ozone Research and Monitoring Project, Report 47, 2003.